Solid State Ionics 288 (2016) 94–97

Contents lists available at ScienceDirect

Solid State Ionics

journal homepage: www.elsevier.com/locate/ssi

Structural and electrical properties of spark plasma sintered scandia- and dysprosia-stabilized zirconia

R.L. Grosso [a,*], A.J. Tertuliano [b], I.F. Machado [b], E.N.S. Muccillo [a]

[a] Energy and Nuclear Research Institute, PO Box 11049, Sao Paulo, SP 05422-970, Brazil
[b] Polytechnique School, University of Sao Paulo, Sao Paulo 05508-010, Brazil

ARTICLE INFO

Article history:
Received 13 July 2015
Received in revised form 12 November 2015
Accepted 13 November 2015
Available online 26 November 2015

Keywords:
Zirconia–scandia
Spark plasma sintering
Densification
Electrical conductivity

ABSTRACT

Zirconia–10 mol% scandia–1 mol% dysprosia solid solution was prepared by the coprecipitation method assisted by spark plasma sintering aiming to verify the densification and the electrical conductivity of the solid electrolyte. Full stabilization of the cubic phase at room temperature was evidenced by room temperature X-ray diffraction. The consolidation technique allowed for obtaining high relative density (>97% of the theoretical value) specimens at low temperatures (1100–1300 °C) with average grain sizes in the submicrometer–micrometer range depending on the sintering temperature. The average grain size is 4.76 μm after consolidation at 1300 °C for 4 min. The total electrical conductivity reached 3.6 mS·cm^{-1} at 650 °C.

1. Introduction

Among the zirconia-based solid electrolytes exhibiting high ionic conductivity, those fully stabilized with yttria and with scandia have been intensively investigated. Their ionic conductivity at 1000 °C amounts 0.12 (9 mol% Y_2O_3) and 0.25 S.cm^{-1} (10 mol% Sc_2O_3) [1,2]. Moreover, these materials show low electronic conductivity, wide electrolytic domain, and high chemical stability. Hence, fully stabilized zirconia solid electrolytes are candidates for a number of technological devices, such as solid oxide fuel cells (SOFCs) and electrolyzers [2,3].

The phase diagram of the zirconia–scandia system consists of several crystalline phases: monoclinic (m), tetragonal (t, t'), cubic (c), and three modifications (β, γ, δ) with rhombohedric structure [4]. The highest ionic conductivity is found in the cubic phase field for scandia content of about 10 mol%. However, on cooling down from the sintering to the room temperature, the reversible cubic ↔ rhombohedric phase transition occurs, giving rise to a relatively low ionic conductivity material. One approach to fully stabilize the cubic structure at room temperature is by the introduction of a second dopant. In this context, addition of rare-earth oxides has been the preferred choice [5–10].

The sintering of zirconia-based solid electrolytes is frequently carried out at temperatures of at least 1350 °C, to obtain dense ceramics with suitable properties [11]. In particular, zirconia–scandia solid electrolytes (with and without a second dopant) have been sintered at even higher temperatures (1500–1700 °C) [5–9,12,13].

Recently, spark plasma sintering (SPS) has emerged as an alternative method to obtain polycrystalline materials with high densification along with fine grain sizes [14]. Regarding codoped systems, the effect of spark plasma sintering was investigated for zirconia–scandia–ceria [15]. The ionic conductivity of spark plasma sintered zirconia–10 mol% scandia–1 mol% ceria was shown to decrease with increasing the dwell temperature, with formation of the tetragonal phase. This effect was attributed to the reduction of Ce^{4+} to Ce^{3+} during sintering.

In a previous work, we have investigated the effect of dysprosium oxide addition to commercial zirconia–10 mol% scandia powder [16]. It was found that the solid electrolyte prepared by solid-state reaction requires a minimum amount of 2 mol% of Dy_2O_3 for full stabilization of the cubic structure at room temperature. In contrast, for chemically synthesized powders, 1 mol% of the additive was effective for phase stabilization [10]. This rare earth was chosen because its ionic radius in 8-fold coordination (1.03 Å) is close to those of yttrium (1.02 Å) and cerium (0.97 Å) and due to its stable valence at the operating conditions of SOFCs.

In this work, the effects of spark plasma sintering on structure and ionic conductivity of chemically synthesized zirconia–10 mol% scandia–1 mol% dysprosia is investigated, aiming to obtain high densification and to evaluate the electrical conductivity of the solid electrolyte.

* Corresponding author at. Department of Chemical Engineering and Materials Science, University of California, Davis, Davis, CA 95616, USA. Tel.: +55 11 31339203: fax: + 55 11 31339276.
E-mail address: roblopeg@usp.br (R.L. Grosso).

http://dx.doi.org/10.1016/j.ssi.2015.11.015
0167-2738/

2. Experimental

2.1. Specimen preparation

Zirconyl nitrate hydrate (99.9%, Aldrich), scandium (III) nitrate hydrate (99.9%, Alfa Aesar), and dysprosium (III) nitrate pentahydrate (99.9%, Alfa Aesar) were used as starting materials for the synthesis by the simultaneous precipitation method of zirconia with nominal additions of 10 mol% scandia and 1 mol% dysprosia. Details on this method and specific parameters of the synthesis may be found elsewhere [10]. The dried precipitate was deagglomerated in an agate mortar and calcined at 500 °C for 2 h. The particle size distribution obtained from images collected by transmission electron microscopy is relatively narrow (37% of dispersion), with an average size of 4.8 nm.

Consolidation of cylindrical specimens was accomplished by spark plasma sintering (SPS 1050, Sumitomo Coal Mining Co., Japan). In a typical sintering cycle, the powder was loaded into a graphite die lined with graphite sheets. The die containing powder was heated up to a specific temperature (1000–1300 °C), with simultaneous application of pressure by a pre-set program. The applied pressure (65 MPa) was released at the end of the holding time, which was fixed at 4 min. Heating and cooling rates in SPS experiments were 100 and 300 °C·min^{-1}, respectively. A subsequent heat treatment at 900 °C for 5 min was performed to eliminate traces of carbon contamination from the die.

2.2. Characterization methods

Structural characterization was accomplished by room temperature X-ray diffraction (Bruker-AXS, D8 Advance) with Ni-filtered Cu K_α radiation in the 20°–80° 2θ range, with 0.05° step size and 2 s time per step. The pellet density was determined by the immersion method with distilled water. The morphology of sintered specimens was observed by field emission scanning electron microscopy, FESEM (FEI, Inspect F50) on polished and thermally etched surfaces. The average grain size was determined by the intercept method on a population of about 1000 grains. The electrical conductivity was determined by electrochemical impedance spectroscopy using an LF-impedance analyzer (HP 4192A) in the 5 Hz–13 MHz frequency range. Resistance values were collected in the 300–800 °C range with 200 mV of applied signal on platinum-coated specimens with 9.8 mm diameter and 0.7–1.0 mm thickness. For comparison purposes, electrical conductivity measurements were also performed in ZrO_2: 10 mol% Sc_2O_3, ZSC (Daiichi Kigenso Kagaku Kogyo, Japan), pressed into discs and sintered at 1550 °C for 10 h.

3. Results and discussion

3.1. Structure and microstructure

Fig. 1 shows the room temperature XRD patterns of spark plasma sintered specimens, obtained after SPS experiments followed by the heat treatment at 900 °C for 5 min. Diffraction patterns were also recorded in as-sintered specimens, but no difference was noted in the diffraction patterns relative to those in Fig. 1. All diffraction profiles are characteristics of the cubic fluorite-type phase (JCPDS 89-5483, *Fm3m* space group), and no other reflections due to tetragonal, rhombohedric or monoclinic phases were detected.

Specimens prepared with ZSC powder, on the other hand, exhibit typical reflections of the β-rhombohedric phase (JCPDS 51-1604, *R3* space group).

Table 1 lists values of the relative density and average grain size of sintered specimens prepared with synthesized powder (S) and the ZSC powder. The specimen sintered at 1000 °C for 4 min reached 81.6% of relative density, but that value increases to about 97% at 1100 °C, and no significant increase is observed with further increase of the temperature up to 1300 °C. The ZSC specimen sintered conventionally at 1550 °C for 10 h attained similar relative density (97.5%) as

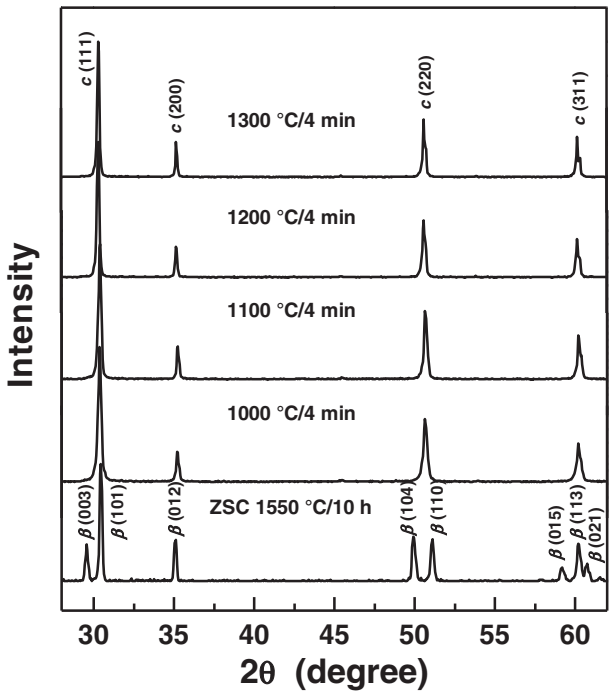

Fig. 1. Room temperature XRD patterns of sintered specimens.

specimens sintered by spark plasma. The average grain size increases with increasing the sintering temperature, as expected. The average grain sizes are in the submicrometer range for specimens consolidated at 1000 and 1100 °C (Table 1). The grain growth is accelerated in the 1000–1200 °C range, but this process slows down with further increase of the dwell temperature.

Typical microstructures of sintered solid electrolytes are shown in Fig. 2 for specimens prepared with (a) ZSC powder and (b) with synthesized powder after SPS at 1300 °C for 4 min. The ZSC specimen (a) exhibits large grains and extensive porosity. The pores are preferentially found intra-grains, although a small fraction of pores still remains at the grain boundaries. For this specimen, a herringbone structure characteristic of the cubic-to-rhombohedric phase transition is seen inside most of the grains [4]. The specimen consolidated by SPS shows polyhedral grains with both intra- and intergrain pores. The latter are mostly found at triple grain junctions. The herringbone structure is not observed in spark plasma sintered specimens. These results are in general agreement with XRD patterns (Fig. 1).

3.2. Electrical conductivity

The electrical conductivity of ZSC and zirconia–10 mol% scandia–1 mol% dysprosia sintered specimens was determined in the 300–800 °C range. In the low temperature range (up to approximately 600 °C), the grain and grain boundary contributions to the overall electrolyte conductivity could be determined without ambiguity. In the high

Table 1
Values of relative density, average grain size, and total electrical conductivity (σ) at 650 °C of sintered specimens. S and ZSC stand for specimens prepared with synthesized and commercial powders.

Specimen-sintering profile	Relative density (%)	Average grain size (μm)	σ (at 650 °C) (mS·cm^{-1})
S-1000 °C/4 min	81.6 ± 0.5	0.18 ± 0.01	–
S-1100 °C/4 min	97.0 ± 0.2	0.81 ± 0.02	1.2
S-1200 °C/4 min	97.5 ± 0.2	3.63 ± 0.36	3.0
S-1300 °C/4 min	97.5 ± 0.1	4.76 ± 0.59	3.6
ZSC-1550 °C/10 h	97.5 ± 0.9	7.75 ± 0.25	17.6

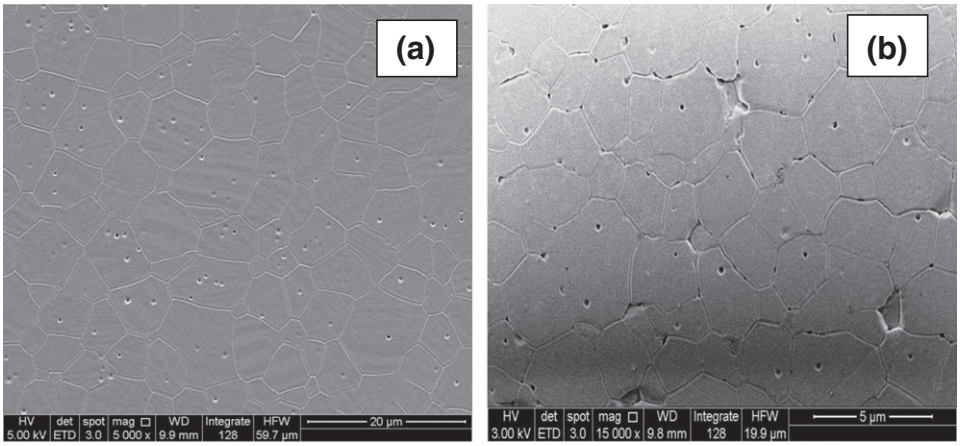

Fig. 2. Representative FESEM micrographs of (a) ZSC (sintered at 1550 °C/10 h) and (b) S (spark plasma sintered at 1300 °C/4 min) specimens.

temperature range (above approximately 600 °C), only the total electrolyte conductivity could be determined. Fig. 3 shows the evolution of the impedance spectroscopy diagrams at selected measuring temperatures for the specimen sintered at 1300 °C for 4 min. In the impedance diagrams at low temperatures, two semicircles along with a spike are easily identified. At 500 °C, the high-frequency semicircle attributed to the grain conductivity is no longer detected due to instrumental limitations.

The magnitude of the grain boundary blocking effect, responsible by the semicircle at intermediate frequencies, decreases continuously with increasing temperature. Similar results were obtained for other specimens consolidated at lower dwell temperatures.

The Arrhenius plots of the grain and the grain boundary conductivities at low temperatures of SPS specimens are shown in Fig. 4. The grain conductivity (Fig. 4a) is essentially unchanged with the dwell temperature. The grain boundary blocking effect (Fig. 4b) decreases with increasing the dwell temperature. Fig. 4c shows the evolution of the specific grain boundary conductivity obtained by normalization by the grain size. It can be seen that the specimen with smallest average grain size exhibits higher specific conductivity. This result suggests that the grain growth process in zirconia–scandia-based electrolytes is accompanied by significant changes in the grain boundaries.

The temperature dependence of the total electrolyte conductivity is depicted in Fig. 5. In this case, the total electrical conductivity of the ZSC specimen sintered at 1550 °C/10 h is also shown for comparison purposes. At high temperatures, all zirconia–scandia–dysprosia specimens display a total electrical conductivity lower than that of zirconia–scandia, similarly to other codoped systems [5–9].

Activation energy values are the same for both zirconia–scandia–dysprosia and ZSC specimens: 1.40 eV (up to 550 °C) and 0.80 eV (550–800 °C). Values of the total electrical conductivity at 650 °C are summarized in Table 1. The electrical conductivity value (1.2 $mS \cdot cm^{-1}$) obtained for the specimen containing 2 mol% dysprosia prepared by solid-state reaction [16] is lower than those for specimens consolidated by SPS at 1200 and 1300 °C. At high temperatures (above 600 °C), the electrical conductivity of ZSC specimen is higher than those of zirconia–scandia–dysprosia solid electrolytes. Specimens sintered at 1200 and 1300 °C exhibit similar electrical conductivity values, which are higher than that of the ZSC specimen in the low temperature range, because of the cubic

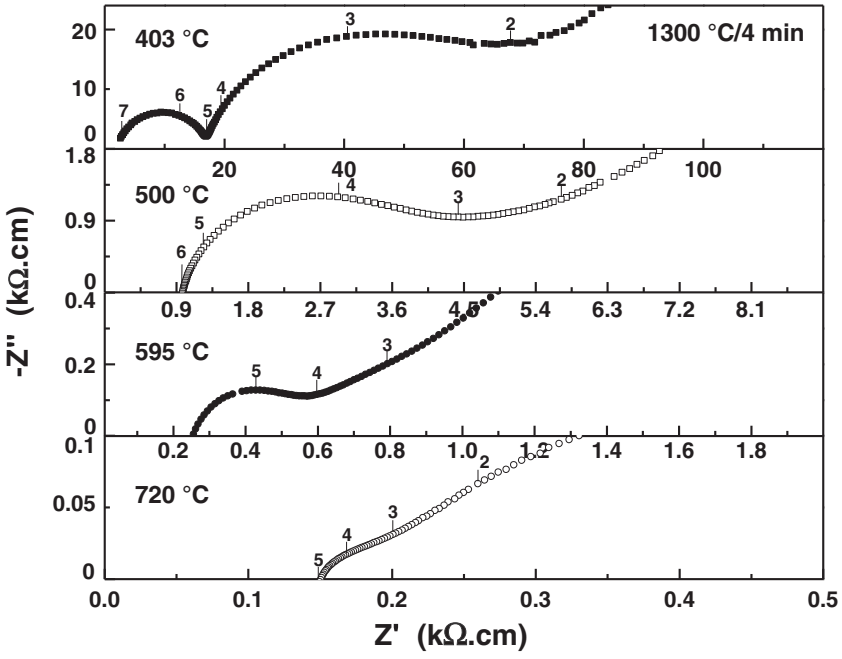

Fig. 3. Impedance spectroscopy diagrams at selected temperatures of the specimen consolidated by SPS at 1300 °C.

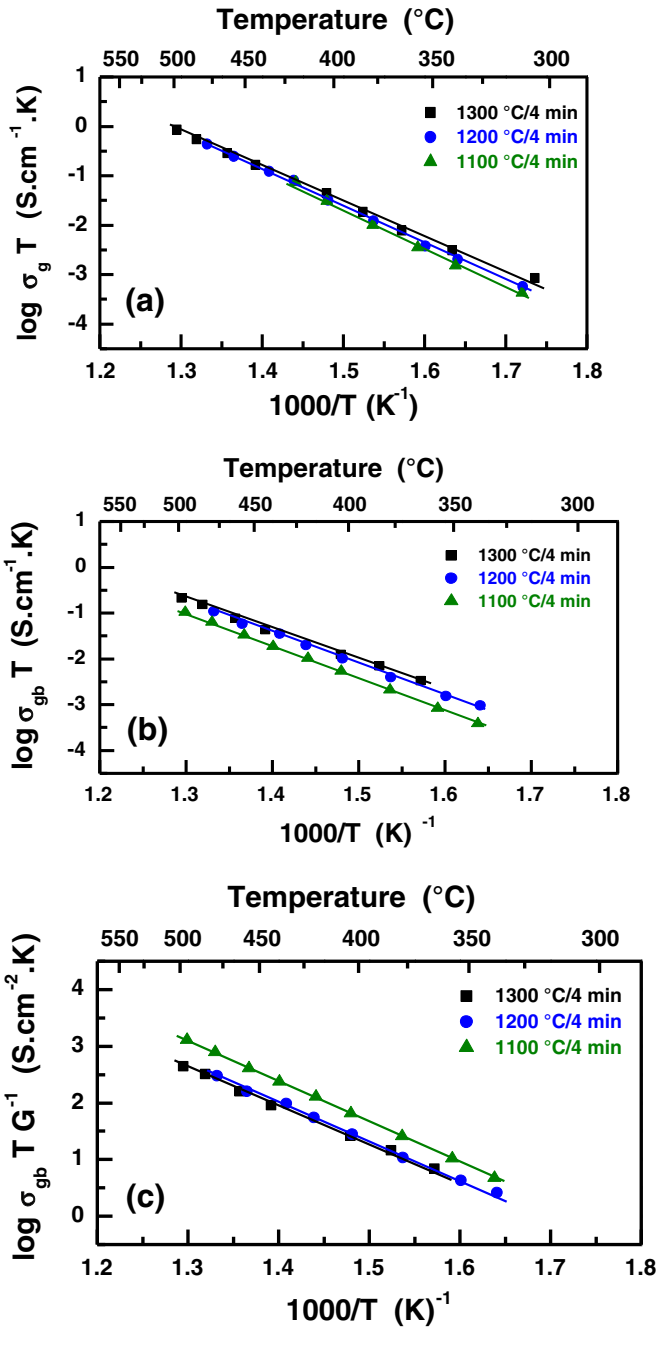

Fig. 4. Arrhenius plots of (a) grain conductivity, (b) grain boundary blocking effect, and (c) specific grain boundary conductivity of zirconia–10 mol% scandia–1 mol% dysprosia specimens consolidated by SPS.

phase stabilization. Nevertheless, these conductivity values are lower than those of zirconia–scandia codoped with ceria (20 mS·cm^{-1} [5]) and yttria (15 mS·cm^{-1} [9]) at the same temperature.

The overall results are a further evidence of the feasibility of the SPS technique to consolidate low-sinterability solid electrolytes avoiding excessive grain growth, and allowing for obtaining high densification at milder processing conditions, without degradation of the electrical properties.

4. Conclusions

Zirconia–10 mol% scandia–1 mol% dysprosia solid electrolyte with high densification (≥97% of the theoretical value) was obtained by spark plasma sintering at relatively low temperatures (1100–1300 °C). The average grain sizes increases with the dwell temperature. The electrical conductivity of specimens prepared by SPS is similar to those of other codoped systems. The cubic phase stabilization at room temperature is responsible for obtaining higher electrical conductivity than that of zirconia–10 mol% scandia in the low temperature range.

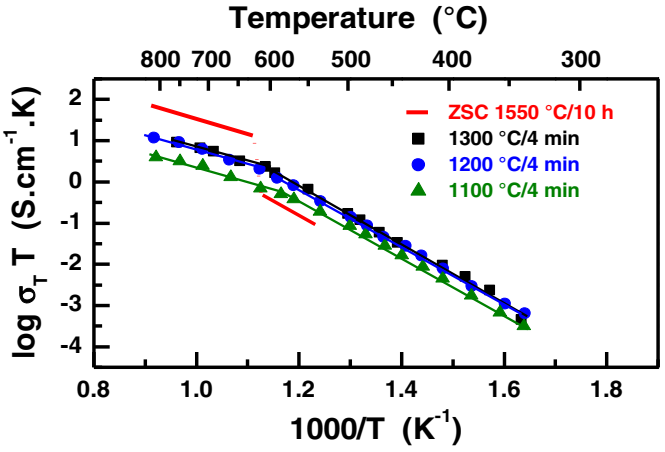

Fig. 5. Temperature dependence of the total electrical conductivity of spark plasma sintered zirconia–10 mol% scandia–1 mol% dysprosia and zirconia–10 mol% scandia specimens.

Acknowledgments

The authors acknowledge FAPESP (2013/07296-2), CNPq (304073/2014-8), and CNEN for financial supports and Daiichi Kigenso Kagaku Kogyo for providing the zirconia–scandia powder. One of the authors (R.L.G.) acknowledges FAPESP (proc. no. 12/03319-5) for the scholarship.

References

[1] T.H. Etsel, S.N. Flengas, Chem. Rev. 70 (1970) 339–376, http://dx.doi.org/10.1021/cr60265a003.
[2] P. Hagenmuller, W. van Gool (Eds.), Solid Electrolytes—General Principles, Characterization, materials, applications, Academic Press, New York, 1978.
[3] E.C. Subbarao, Solid electrolytes and their applications, Plenum, New York, 1980.
[4] R. Ruh, H.J. Garret, R.F. Domagala, V.A. Patel, J. Am. Ceram. Soc. 60 (1977) 399–403, http://dx.doi.org/10.1111/j.1151-2916.1977.tb.15521.x.
[5] Z. Wang, M. Cheng, Z. Bi, Y. Dong, H. Zhang, J. Zhang, Z. Feng, C. Li, Mater. Lett. 59 (2005) 2579–2582, http://dx.doi.org/10.1016/j.matlet.2004.07.065.
[6] T. Ishii, T. Iwata, Y. Tajima, A. Yamaji, Solid State Ionics 57 (1992) 153–157, http://dx.doi.org/10.1016/0167-2738(92)90078-4.
[7] S. Omar, W.B. Najib, W. Chen, N. Bonanos, J. Am. Ceram. Soc. 95 (2012) 1965–1972, http://dx.doi.org/10.1016/j.ssi.201009.042.
[8] O. Yamamoto, Y. Arati, Y. Takeda, Y. Imanishi, N. Mizutani, M. Kawai, Y. Nakamura, Solid State Ionics 79 (1995) 137–142, http://dx.doi.org/10.1016/0167-2738(95)00044-7.
[9] T.I. Politova, J.T.S. Irvine, Solid State Ionics 168 (2004) 153–165, http://dx.doi.org/10.1016/j.ssi.2004.02.007.
[10] R.L. Grosso, J.R. Matos, E.N.S. Muccillo, J. Therm. Anal. Calorim. 117 (2014) 567–572, http://dx.doi.org/10.1007/s10973-014-3766-7.
[11] I.R. Gibson, G.P. Dransfield, J.T.S. Irvine, J. Mater. Sci. 33 (1998) 4297–4305, http://dx.doi.org/10.1023/A:1004435504482.
[12] S.P.S. Badwal, F.T. Ciacchi, D. Milosevic, Solid State Ionics 136 (137) (2000) 91–99, http://dx.doi.org/10.1016/S0167-2738(00)00356-8.
[13] Y. Arachi, T. Asai, O. Yamamoto, Y. Takeda, N. Imanishi, K. Kawate, C. Tamakoshi, J. Electrochem. Soc. 148 (5) (2001) A520–A523, http://dx.doi.org/10.1149/1.1366622.
[14] Z.A. Munir, D.V. Quach, M. Ohyanagi, J. Am. Ceram. Soc. 94 (1) (2011) 1–19, http://dx.doi.org/10.1111/j.1551-2916-201004210.x.
[15] R.L. Grosso, M. Bertolete, I.F. Machado, R. Muccillo, E.N.S. Muccillo, Solid State Ionics 230 (2013) 48–51, http://dx.doi.org/10.1016/j.ssi.2012.08.006.
[16] R.L. Grosso, E.N.S. Muccillo, ECS Trans. 61 (1) (2014) 341–346, http://dx.doi.org/10.1149/061.01.0341ecst.